

Original Research Article

Biochemical and Histopathological Effects of Chitosan-Selenium Nanoparticles in Experimentally Induced Diabetic Type-2 in Male Rat

Sura Mahmoud Hamza^{1*}, Ahmed Obied¹, Haider Turky Mousa Al-Mousawi¹

¹Applied Biotechnology, College of Biotechnology, Al-Qasim Green University, Babylon 51013, Iraq

***Corresponding Author:** Sura Mahmoud Hamza

Applied Biotechnology, College of Biotechnology, Al-Qasim Green University, Babylon 51013, Iraq

Article History

Received: 17.11.2025

Accepted: 09.01.2026

Published: 12.01.2026

Abstract: **Background:** Type 2 diabetes mellitus (T2DM) is a metabolic disease that is lifelong and is associated with hyperglycemia, oxidative stress, and other dysfunctions of the organs. The antioxidant effect and bioavailability of selenium nanoparticles have been of interest, particularly whereby the nanoparticles have been stabilized using biocompatible polymers such as chitosan. **Aim:** The study in question was aimed at comparing the effects of metformin and chitosan-selenium nanoparticles (Cs-Se NPs) on biochemical and histopathological levels in an experimental model of type 2 diabetes in rats induced artificially. **Materials and Methods:** One hundred albino adult rats were separated into 6 groups i.e. control negative, control positive (alloxan induced diabetes), 1.5, 3 and 5mg/kg SCNP treated diabetic and a 500mg/kg metformin treated diabetic group. Alloxan was used to induce diabetes. The UV-Vis spectroscopy, XRD, FTIR, SEM, and AFM were used to characterize and synthesize Cs-Se NPs. **Findings:** The diabetic rats with Alloxan exhibited considerable serum urea, creatinine, liver enzymes, HbA1c, total cholesterol, triglycerides, and LDL increases and a significant decrease in HDL. Cs-Se NPs treatment caused the most significant dose-related changes in all the biochemical parameters with the dose of 5 mg/kg showing the most significant protective effects, which were similar or even more effective than metformin. **Conclusion:** Chitosanselenium nanoparticles are powerful antidiabetic agent, antioxidant agent, and organ-protective agent in alloxan-induced type 2 diabetic rats. The increased doses of Cs Se NPs proved to be more effective and thus it can be pointed out that they can serve as an effective nanotherapeutic approach in the management of diabetes and its complications.

Keywords: Diabetes mellitus, Nanoparticles, Chitosanselenium nanoparticles.

INTRODUCTION

The patient is persistently hyperglycemic in diabetes mellitus, a metabolic disorder, which may involve either insulin secretion, or insulin action, or both. It is one of the most typical non-communicable diseases on the planet and has a significant burden on the healthcare systems affecting hundreds of millions of individuals. Besides the condition being one of the most common causes of death and disability, it also predisposes individuals to cardiovascular disease, kidney failure, and blindness (Zheng *et al.*, 2018). Both fixed and modifiable factors are the risk factors of type 2 diabetes mellitus (T2DM). Examples of the modifiable risk factors include age, race/ethnicity, family history, and hereditary susceptibility. A higher risk is posed to South Asians, African-Americans, and Hispanics, e.g. (Nguyen *et al.*, 2022; Khera *et al.*, 2023). In contrast to other essential trace elements, selenium (Se) reacts with proteins as their cofactor and can be potentially applied in the treatment and prevention of certain disorders (Chen *et al.*, 2020; Barchielli *et al.*, 2022). This micronutrient metalloid is the main constituent of enzymes that depend on its presence to be active, e.g. glutathione peroxidase (GSH-Px). Moreover, a large number of epidemiological studies have demonstrated that certain diseases are linked to the lack of Se (Ye *et al.*, 2021). The selenium-dependent glutathione peroxidases (Se-GSH-Px) activation by SeNPs was once considered the explanation of the new in vitro and in vivo antioxidant properties (Mohamed *et al.*, 2021). Moreover, Se-NPs are sevenfold lower toxic to mice and acutely than sodium selenite and threefold lower toxic than organic Se (DeDiego *et al.*, 2024). And not to mention the fact that the SeNPs have been shown to reduce the level of blood sugar (Al-Quraishy

Copyright © 2026 The Author(s): This is an open-access article distributed under the terms of the Creative Commons Attribution 4.0 International License (CC BY-NC 4.0) which permits unrestricted use, distribution, and reproduction in any medium for non-commercial use provided the original author and source are credited.

Citation: Sura Mahmoud Hamza, Ahmed Obied, Haider Turky Mousa Al-Mousawi (2026). Biochemical and Histopathological Effects of Chitosan-Selenium Nanoparticles in Experimentally Induced Diabetic Type-2 in Male Rat. *South Asian Res J App Med Sci*, 8(1), 1-11.

et al., 2015; Das *et al.*, 2025). Much research has shown the correlation of low serum selenium and type 2 diabetes, possibly due to the strong antioxidant and anti-inflammatory properties of selenium. The relationship between a higher level of selenium and reduced risk of having type 2 diabetes has been identified by multiple studies (Wongdokmai *et al.*, 2021). Deacetylation also produces chitosan that is the second most common polymer in the world and found on the cell walls of fungi and crustaceans. The units of the linear polysaccharide are linked together by glycosidic bonds of glucosamine and N- acetylglucosamine. The functional amino and hydroxyl groups offer numerous opportunities to chemically modify it, stabilize nanoparticles, and conjugate drugs to it (Dash *et al.*, 2011). Due to ITS efficiency, low cost, and favorable safety profile, metformin is the initial intervention therapy of Type 2 Diabetes Mellitus (T2DM) and is administered orally to regulate the amount of sugar in the bloodstream. Solini and Tricò (2024) state that this biguanide molecule primarily reduces the level of fasting plasma glucose by reducing the hepatic gluconeogenesis. It achieves this without causing an expansion in insulin production which significantly reduces chances of hypoglycemia. We sought to determine whether the CTS-Se-NPs could exhibit hypoglycemic effect, reduce hepatic and renal injury or even increase the therapeutic action of metformin *in vivo*, thus we intended to develop new therapeutic interventions that could alleviate the complication of DM by using stabilized CTS-Se-NPs and MET.

MATERIALS AND METHODS

Chemicals

All the chemicals used were provided by Sigma- Aldrich, and they were of analytical grade. Alloxan came in Sigma Chemicals of St. Louis, USA. All of the functional solutions were made using deionized water.

Nanoparticles Synthesis

Combine 5 milliliters of acetic acid and 495 milliliters of distilled water at 45 °C. Into 50 milliliters of water add 0.5 grams of chitosan and 6.0 grams of ascorbic acid. To 385 milliliters of the above chitosan 0.5 gram of selenite salt was dissolved in 25 milliliters of distilled water with constant stirring. Add distilled water in order to make it 500 ml. Filter the solution using filter papers. Then, bake it at 40 °C for a few days. To dry it, one can use the dry freezing method, and it includes freeze drying. The solution is dried to form a Selenium-chitosan nanoparticles powder (Bai *et al.*, 2017).

Animals

The animal house at the Al-Qasim green university college of veterinary medicine supplied sixty (60) albino rats that weighed 200-1900 grams. The animals were housed in specially designed plastic cages that had metal mesh lids and fitted with sawdust, and the watering system. The enclosures were sanitized and kept in order. The experimental animals were maintained under the ideal laboratory environment at a range of temperatures between 20-25 °C.

Induction of Diabetes Type 2

The alloxan was obtained at Sigma-Aldrich of St. Louis, MO, USA. Rats that were overnight starved were injected intraperitoneally with the fresh solution at the rate of 150mg/kg after it was dissolved in an 85% phosphate buffer solution with pH of 4.5. The Accu-Check Active Blood Glucometer Kit Roche Diabetes Care Pvt Ltd. in Mumbai, India was used to measure the level of blood sugar seven days after induction. The criteria used in the previous studies (Thomasset *et al.*, 2007; Ibrahim *et al.*, 2018) was diabetic condition, which refers to the presence of glucose in the blood above 250mg/dL.

Selenium-Chitosan nanoparticles characterization Characteristics of the nanoparticles. This powder was studied with diverse methods which included X-Ray diffraction, Atomic Force Microscopy, Fourier Transform Spectrophotometry, UV-Visible Absorption spectrophotometry and scanning electron microscopy.

Experimental Design

First Group (Negative Control): The animals received normal saline orally during the experiment period (60 day).

Second Group (Positive Control): Alloxan injections (150mg/kg in 3 days) to cause diabetes. Without any treatment.

Third Group (CsSe NPs 1): Diabetic animals were subjected to treatment of 1.5 mg of chitosan-selenium nanoparticles orally on a 60-day consecutive basis.

Fourth Group (Cs NPs 2): Animals with induced diabetes were subjected to oral delivery of 3.0 mg of chitosan selenium nanoparticles (concentration) in 60 consecutive days.

Five Groups (Cs-Se NPs 3): Diabetic animals were administered concentration of 5.0 mg of chitosan-selenium nanoparticles at the oral cavity after the administration of 60 consecutive days.

Sixth Group (ME): The animals treated with metformin (500 mg/kg) as a chemical treatment orally over 60 days in a row induced diabetes.

Blood Sampling

At the expiry of 60 days the experiment the animals were starved after which blood samples were drawn by (heart puncher) and the blood was added in gel tubes and put in an incubator at 37 degrees within 30 minutes. Then, the centrifuge

was performed at a speed of 3000 rpm and lasted 15 minutes to separate the serum with the rest of the components using a micropipette and stored in an Eppendorf tube and locked in the refrigerator until it was used.

Biochemical Assessments

The level of serum creatinine was assessed with the help of a commercially available kit (Bioassay Laboratory Technology, Chain). Measurement of blood urea nitrogen (BUN) was done using a commercially available kit of (Elabscience, China). The serum liver enzymes (GOT and GPT) were measured using kit that is sold commercially (Elabscience, China) (Aboktifa *et al.*, 2025). Assessment of glycated hemoglobin (hpA1c). To quantify glycated hemoglobin A1c, fresh blood samples were quantified with the help of a Genru PA120 Analyzer. The analysis was done within 30 minutes after the thawing of the frozen serum which was then spin at a rate of 3000 rpm at 20 minutes. The supernatants were immediately collected and analysed without passing through any freeze-thaw cycles. Combine 10 μ L of serum with 1 mL of reagent following incubation at 37 $^{\circ}$ C over 10 minutes. The readings were then recorded at 450 nm against a blank. The samples were stored at room temperature (20 $^{\circ}$ C-25 $^{\circ}$ C) prior to analysis in line with the procedure described by Al-Tamimi *et al.*, (2024).

Lipid Profile Analysis

Randox kits that were used to test the total cholesterol, triglycerides and the HDL-cholesterol included Randox Laboratories Ltd., Antrim, UK. The level of lipoprotein cholesterol and extremely low-density-lipoproteins cholesterol was calculated as Friedewald *et al.*, (1972) and Dnan *et al.*, (2025) did.

Histopathological Aspect

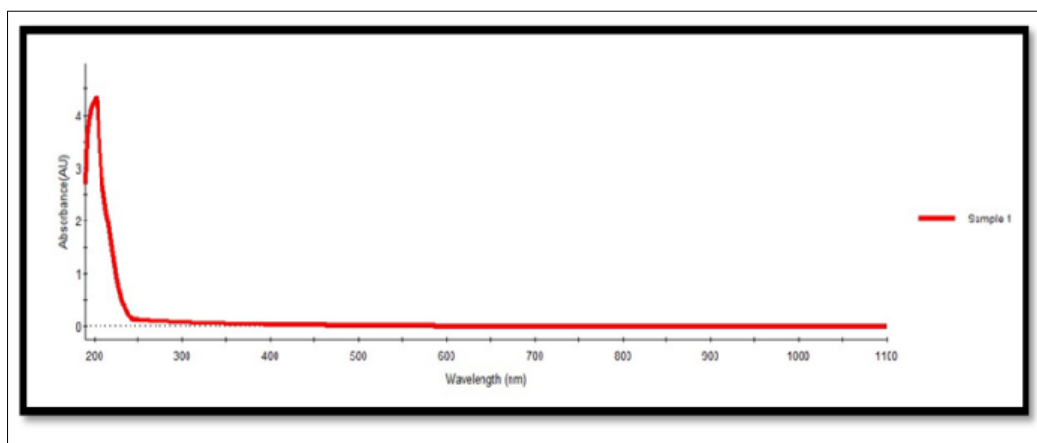
The animals were beheaded and then killed humanely and their inner organs (liver, kidneys and pancreas) were stored under 10 percent neutral buffered formalin saline (72 hours). In the case of light microscopy analysis, the tissues were fixed in paraffin and cut in 5-sections. All the slices were stained with a hematoxylin-eosin (H&E) stain as per Luna (1968) and Malik *et al.*, (2022).

Statistical Analysis

The results of this study have been reported in the form of the mean and the mean deviation ($n = 10$). Al-Rekabi *et al.*, (2021) analyzed the data in SPSS 8 software that contained a one-way analysis of variance (ANOVA) and a Tukey post hoc test (HSD) that made multiple comparisons.

RESULTS

Characterization of 1-Selenium chitosan nanoparticles (Cs-Se NPs) 1-Selenium chitosan (Cs-Se NPs) is a nanoparticle that can be characterized through several different methods. Characterization of 1-Selenium chitosan nanoparticles (Cs-Se NPs) 1-Selenium chitosan (Cs-Se NPs) is a nanoparticle which can be characterized in a number of different ways. UV-visible spectroscopy was used in order to confirm the formation of Cs-Se NPs. Its maximum absorbance is found in the range of 200-250 nm as observed in Figure 1. These findings are in agreement with those made by Desouky *et al.*, (2025). In line with the results established by Lin and Chris Wang (2005), that the size of the particle is related to the nature of the UV-visible spectra, these findings helped to clearly indicate that all selenium nanoparticles were less than 100 nm. Moreover, particles that were 100 nm and below in diameter had a characteristic peak in the UV absorption (Lin and Chris Wang, 2005). Ramamurthy *et al.*, (2013) reported that the surface plasmon resonance (SPR) absorption peak of the Se NPs was between 200 and 400 nm.



The analysis of XRD presented in Figure 2 was carried out to determine the crystal structure and the phase composition of chitosan-selenium nanoparticles. The XRD pattern confirms the existence of selenium particles whereby it shows nano-crystalline structure and that is quite congruent to the conventional selenium powder. The crystalline planes (100), (101), (110), (111) and (201) were identified as the clearest ones at (23.2, 29.7, 41.5 and 45.3) and (52.1). In line with the value of the literature (JCPDS File No.06-0362), the computed lattice constants are ($a = 4.38 \text{ \AA}$ and $c = 4.88 \text{ \AA}$). The XRD analysis of chitosan-Selenium nanocomposites provides crystalline structure, unlike the amorphous structure that indicates strong coating of selenium nanoparticles on chitosan. The size of the particles is usually 41 nanometers.

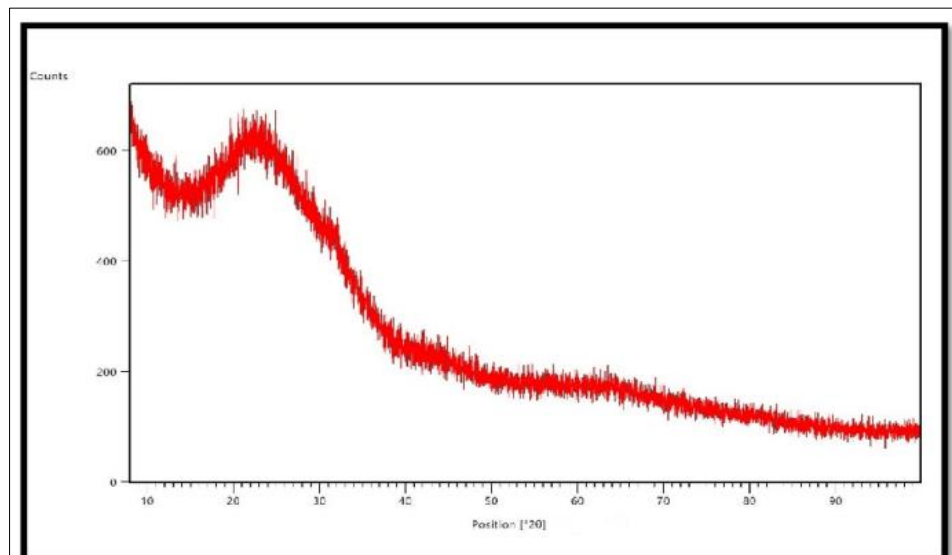


Figure 2: XRD spectrum of Chitosan-Selenium

The reactive functional groups of the produced nanoparticles were examined through the FTIR / fourier transform infrared spectroscopy in the spectral range (4000-450 cm⁻¹). As there were O-H stretching carboxylic acids, a broadband of 3481 cm⁻¹ was observed. The appearance of a narrow band at (2924 cm⁻¹) is suggestive of C-H stretch alkanes. A strong band at 1746–1615 cm⁻¹ that was thin and strong was the amide II band or N 2 H primary amines. There is also C-O-H bending, (1413 cm⁻¹). The C-H bending is linked with (1309 cm⁻¹) band in alkanes. The C-N stretching of the amines are shown by the bars at (1132 cm⁻¹ and 1085 cm⁻¹) in figure 3. The FT-IR results indicate the formation of the chitosan-selenium nanoparticles and capping of the nanoparticles using bio chemicals present in the chitosan. AFM imaging was a vital and rapid study instrument to describe the nanoparticle suspensions and supported the morphology and topography of the surface of the SeNPs (Klapetek *et al.*, 2011).

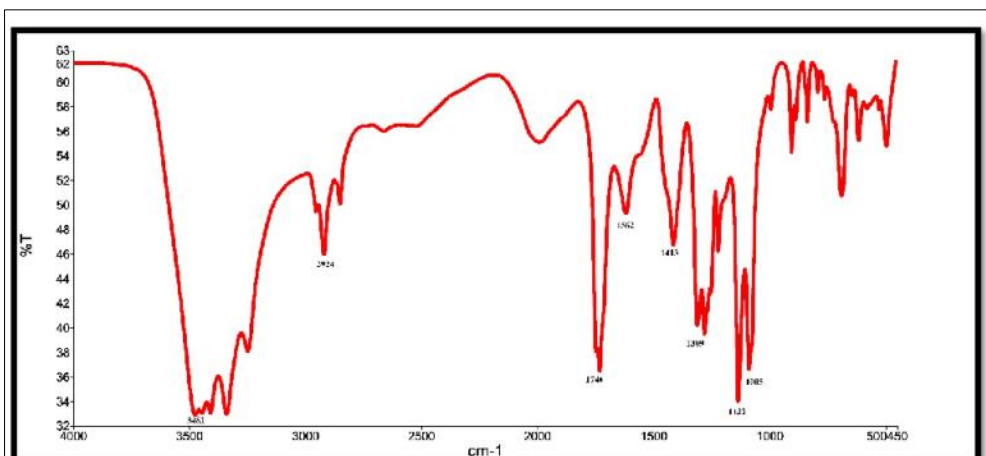


Figure 3: FTIR spectrum of chitosan-selenium nanoparticle

The stability of Selenium nanoparticles by chitosan with an average diameter of 41 nm and a shape that is spherical as illustrated in the SEM analysis in figure 4. This finding is similar to that of Birsan *et al.*, (2022), who found that chitosan

selenium nanoparticles are spherical with a mean of 4060 nm (Birsan *et al.*, 2022). The atomic force microscopy (AFM) has the capability of giving a 2 and 3D profile of the surface at a nanoscale. The synthesized chitosan-Selenium NPs were characterized in the current research by the captured figure of AFM image 5. The atomic force microscopy (AFM) analysis of chitosan-selenium nanoparticles revealed that the polymeric surface was rather smooth and possessed nanoscale aspects throughout the scanned area. The height of the particles was between (24 to 45 nm) with a mean height of 26 nm indicating that there was a relatively narrow size distribution. The surface was not very rough, which means that the coating of chitosan formed a uniform stabilizing layer. The distribution of the nanoparticles was observed to be uniform without any observable aggregation due to the high particle density (greater than (1×10^8) particles/mm²). The particles had the typical morphology of biopolymer-stabilized selenium nanoparticles that is a chitosan matrix infused within oblate or dome-shaped spheres.

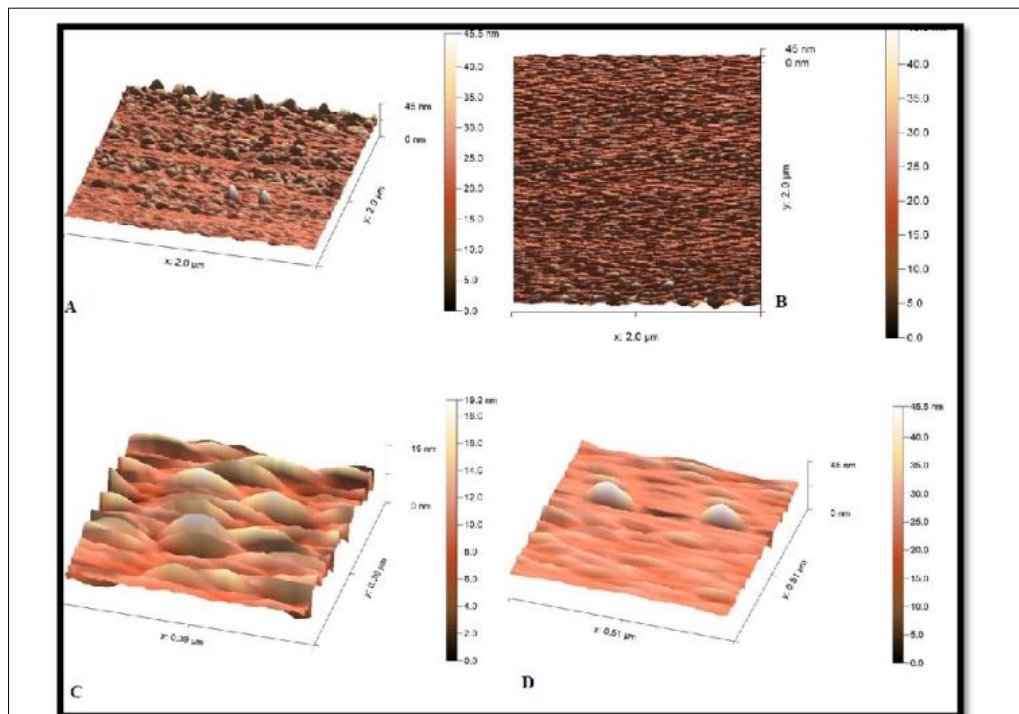


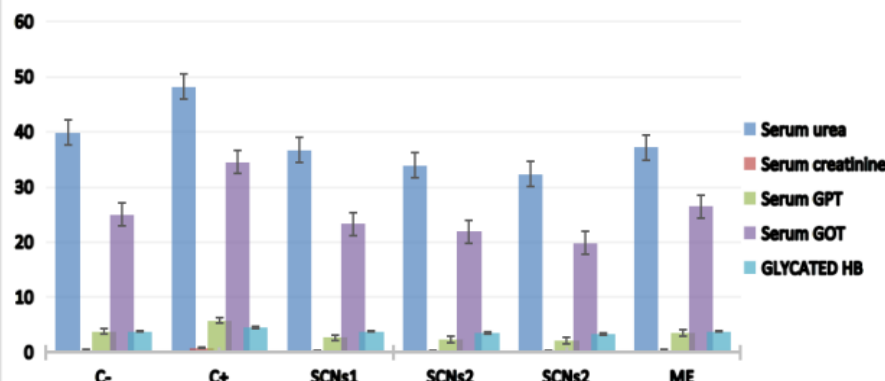
Figure 4: AFM topographical images of the chitosan SeNPs, A and B scan area of SeNPs in 2-D image, C and D scan area of SeNPs in 3-D image.

Biochemical Analysis

In the given research, the findings of serum blood urea nitrogen and creatinine that were demonstrated in table (1) and figure (5) exhibited a significant ($p=0.05$) elevation in control positive (C+) group as compared to the other group. No major dissimilarities were discovered in the same line between control negative group (C-), and metformin group (ME). Although the control negative (C-), Cs-Se NPs 1 group did not have any significant difference when compared to the other groups. Moreover, the creatinine and blood urea nitrogen in diabetic rats treated with (1.5, 3, and 5mg/kg) of Cs became significantly reduced in a dose-dependent manner. In the case of liver enzymes (GOT and GPT), serum, the statistical analysis obtained significant ($p \leq 0.05$) increase in the control positive (C+) group compared to the other group. In addition, there were no major variations in control negative group and metformin group (ME). Although the control negative (C-), Cs-Se NPs 1 group did not have any significant difference when compared to the other groups. Moreover, the diabetic rats which were administered (1.5, 3 and 5mg/kg) of Cs- Se NPs experienced a significant drop in the GOT and GPT in serum in a dose dependent manner as tabulated in table (1) and figure (5). The glycated hemoglobin main value was very high ($p=0.05$) in control positive group that was treated with Alloxan (control group) compared to other treatment groups (C-, ME, Cs NPs1, Cs NPs2, and Cs NPs3) respectively. Conversely, the statistical test did not demonstrate any significant differences between control negative and metformin groups on glycated hemoglobin levels. The current research results showed that the dose-dependent decrease in glycated hemoglobin was significant among animals being exposed to varying doses of Cs Se NPs as shown in table (1) and figure (5).

Table (1): The effect of administering selenium nanoparticles and metformin on some blood and serum parameters

Parameter	C-	C+	SCNs1	SCNs2	SCNs3	ME	LSD
Serum urea	39.86 ± 0.54 B	48.22 ± 1.34 A	36.67 ± 1.67 C	33.91 ± 0.9 D	32.38 ± 0.9 D	37.2 ± 2.62 B	3.142
Serum creatinine	0.43 ± 0.02 B	0.8 ± 0.03 A	0.36 ± 0.05 C	0.31 ± 0.08 D	0.27 ± 0.03 E	0.4 ± 0.04 B	0.04
Serum GPT	3.82 ± 0.09 B	5.8 ± 1.1 A	2.66 ± 0.72 C	2.38 ± 0.09 C	2.1 ± 0.45 C	3.59 ± 0.36 B	0.29
Serum GOT	24.97 ± 1.1 B	34.51 ± 0.84 A	23.35 ± 3.11 C	21.96 ± 2.29 C	19.87 ± 1.88 D	26.44 ± 1.36 B	1.79
Glycated HB	3.81 ± 0.17 B	4.56 ± 0.25 A	3.82 ± 0.03 B	3.5 ± 0.12 C	3.35 ± 0.12 C	3.83 ± 0.05 B	0.21

Biochemical analysis**Figure (5): Biochemical analysis of different treatment groups**

3-Serum Lipids Profile

Table (2) indicates that when Alloxan was administered to the rats, the levels of HDL decreased significantly and those of serum total cholesterol, TG and LDL increased significantly in the animals as compared to the normal group. The metrics mentioned above were enhanced in the diabetic mice using Cs-Se NPs. The current study resulted in that the control positive group had a significantly higher serum cholesterol, triglycerides, and low-density lipoprotein (LDL) than other groups ($p \leq 0.05$). The metformin and control groups do not have a statistically significant difference as well. Figure 6 indicates that the serum HDL of diabetic rats treated with different concentrations of chitosan selenium nanoparticles (Cs-Se NPs) reduced dose-dependently after the statistical analysis ($p=0.05$).

Table (2): The effect of administering selenium nanoparticles and metformin on some lipid profile

Parameter	C-	C+	SCNs1	SCNs2	SCNs3	ME	LSD
Serum Cholesterol	271.20 ± 29.01 B	338.52 ± 13.79 A	251.67 ± 50.02 C	249.60 ± 38.91 C	241.60 ± 35.71 C	278.40 ± 24.21 B	22.24
Serum triglycerides	59.87 ± 45 B	89.51 ± 10.80 A	47.15 ± 3.79 C	44.89 ± 8.06 C	41.24 ± 1.45 C	56.87 ± 1.45 B	8.34
Serum LDL	172.27 ± 21.57 B	200 ± 17.21 A	155.99 ± 29.3 C	151.99 ± 33.3 C	148.54 ± 19.4 C	169.81 ± 34.14 B	10.81
Serum HDL	43.63 ± 7.24 B	20.88 ± 4.53 C	52.46 ± 5.11 A	57.66 ± 8.27 A	58.16 ± 5.36 A	43.75 ± 4.29 B	12.24

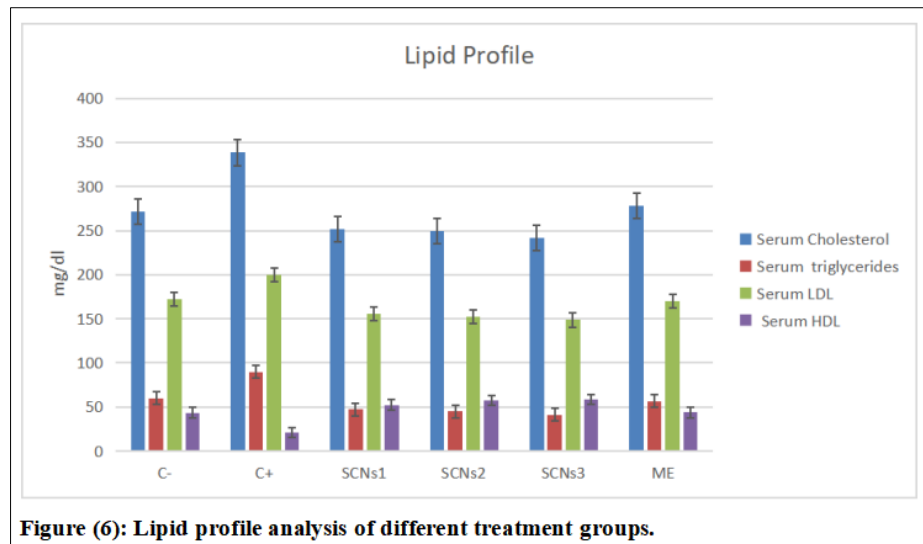


Figure (6): Lipid profile analysis of different treatment groups.

Pancreatic Histopathology

- Control negative group: normal islet of Langerhans, alpha and beta cells blood vessels (fig 7A).
- Control positive group: Varying histopathological changes with necrosis of islet of Langerhans, serous secretory unit vacuolar degeneration, blood vessels congestion with edema (fig 7B).
- Cs-Se NPs1 group in this group inflammatory cells, hyper atrophy of interlobular duct, degeneration of few serous secretory unit (fig 7D).
- CsSe NPs2 group: Stain of pancreatic histopathological section showed normal structure of serous secretory unit, fibrosis, adipose fatty tissue deposition (fig 7E).
- CsSe NPs3 group: normal structure of serous secretory unit, normal pancreatic duct interlobular and intralobular, fibrosis and mildly blood vessels congestion (fig 7F).
- Metformin group: Demonstrates blood vessels congestion, slight degeneration of peripheral of islet of Langerhans, normal structure of serous secretory unit (fig 7C).

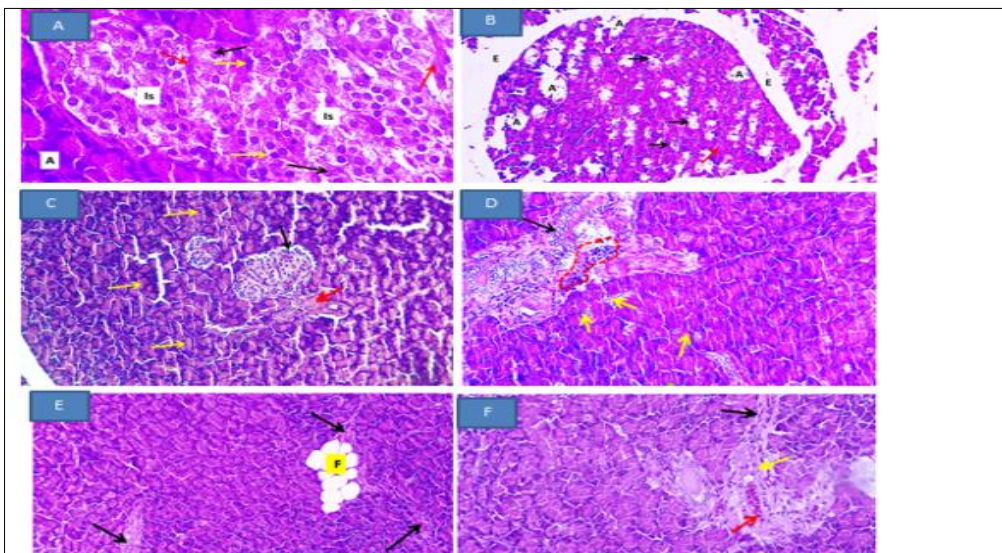


Figure (7): Histological section of pancreas (A) control showing serous unit (A), normal islet of langerhans (Is), blood vessels (red arrow), beta cell (yellow arrow), alpha cell (black arrow). (B) control positive group showing different histopathological changes, necrosis of islet of langerhans (A), vacuolar degeneration of serous secretory unit (black arrow), congestion of blood vessels (red arrow), edema (E). (C) metformin group Showing congestion of blood vessels (red arrow), slight degeneration in the peripheral of islet of langerhans (black arrow), normal structure of serous secretory unit (yellow arrow). (D) Histological section of pancreas selenium 1.5 mg group showing: infiltrations of inflammatory cell (red circle), hyper atrophy of interlobular duct (black arrow), degeneration of some serous secretory unit (yellow arrow). (E) Histological section of pancreas selenium 3mg group Showing: normal structure of serous secretory unit, fibrosis (black arrow), deposition of adipose fatty tissue (F). (F) Histological section of pancreas selenium 5mg group normal structure of serous secretory unit, normal pancreatic duct (interlobular (yellow arrow) and intralobular (blue arrow)), fibrosis (blue arrow), slightly blood vessels congestion (red arrow). H&E stain. X100.

DISCUSSION

The results of the current research provide valuable information about the biochemical changes that occur in alloxan-induced diabetes and the modulating influence of the supplementation of selenium chitosan nanoparticles to various doses in comparison to metformin. The most remarkable finding was the steady and dramatic rise in serum urea, creatinine, GPT, GOT, and HbA1C in the alloxan treated group with a significant drop in HDL levels that all point to the severe metabolism and organ specific toxicity of alloxan. These observations conform to the vast amount of evidence showing that alloxan induces diabetes by specifically killing pancreatic β -cells by the formation of reactive oxygen species (ROS) resulting in insulin deficiency, hyperglycemia, oxidative damage, and systemic metabolic dysfunction (Lenzen, 2008; Szkudelski, 2001). The high increase of urine urea and creatinine in control positive group is the characteristic of the renal impairment caused by the combination of the sustained hyperglycemia, destruction of glomerulonephritis endothelial cells, and oxidative stress contributing to the decrease in glomerular filtration rate and augmented catabolism of proteins (Forbes & Cooper, 2013). Diabetic nephropathy is reported to progress very quickly in chemically induced diabetic models, and oxidative stress is the most dominant in the degeneration of renal structures which is consistent with the observed biochemical alterations (Giacco & Brownlee, 2010). The lack of major differences between control, metformin, and selenium 1.5 mg/kg (Cs-Se NPs 1) of the renal markers are likely evidence that low doses of selenium lacks the necessary reno-protective effect but the much lower levels of urea in the selenium 3 mg/kg and selenium 5mg/kg (Cs Se NPs 3) groups indicates that there is dose dependence in the effect of selenium on renal functions. An increase in the selenium dosage seems to indicate better antioxidant ability, as selenium plays a vital part in the synthesis of selenoproteins, including selenoprotein P, glutathione peroxidase (GPx), and thioredoxin reductase, which protect against oxidative stress and maintain the integrity of renal tissue (Steinbrenner & Sies, 2013). This interpretation is further supported by the high levels of creatinine in the rats treated with alloxan and the gradual decrease with the increase in the doses of selenium. Selenium of 5 mg/kg induced the best effect on the creatinine levels, which indicates a robust nephroprotective effect, ROS scavenging, mitochondrial activity and tubular degeneration improvement which have been reported in various diabetic animal models (Alissa & Ferns, 2012; Rahmanto & Davies, 2012). The massive disparities in selenium dosages lead to a dose responsive effect on the physiological system, as shown by earlier studies that report an effective physical activity of selenium only at levels that correspond to a threshold level of selenoenzyme expression (Hatfield *et al.*, 2014).

The substantial rise in level of GPT and GOT in the alloxan group indicates hepatic damage, which is one of the characteristics of uncontrolled diabetes. Hyperglycemia leads to over hyperglycemia causes excessive fatty acid mobilization, lipid deposition in the hepatocyte, mitochondrial dysfunction, and increased lipid peroxidation, which leads to hepatocellular damage and release of hepatocyte enzymes into the circulation (Bugianesi *et al.*, 2005; Rolo & Palmeira, 2006). It was also revealed that Alloxan has direct oxidative toxicity, which affects antioxidant defenses in the liver, and increases the cell injury (Szkudelski, 2001). The absence of substantial differences between control and metformin groups in GPT and GOT is the support that metformin does not drive hepatic integrity, but rather by its well-documented capacity to increase insulin sensitivity, reducing hepatic glucose manufacture, and countering oxidative stress (Rena *et al.*, 2017). The use of metformin has been reported to lessen the hepatic steatosis as well as to reduce the liver enzyme elevations in diabetic models, as we have observed (Viollet *et al.*, 2012). The dose-dependent effects of selenium on liver enzymes as indicated by its significant differences between selenium 1.5mg/kg and the higher doses also underscore the hepatoprotective effects of selenium. Dose levels of selenium (3 mg/kg and 5mg/kg) had a significant reducing effect on GPT and GOT, which showed an improvement in the reversal of the membrane of the hepatocellular and increased the expression of antioxidant enzymes engaged in degradation of hydrogen peroxide and lipid peroxides. This coincides with the evidence that selenium supplementation inhibits hepatic necrosis, decreases ROS and alters inflammatory responses in diabetic rodents (Zeng *et al.*, 2008; Huang *et al.*, 2012). The enhanced performance of the selenium 5 mg/kg group could be explained by full-scale stimulation of GPx and a better redox status that restrains the hepatocellular oxidative stress and maintains the membrane permeability. Results of the biochemical analysis thus confirm the idea that high doses of selenium can be used as an effective antidote to diabetes-related hepatic dysfunction. The high (there is the anticipation of significantly high HbA1c) in the alloxan group due to the excruciating hyperglycemia caused by the destruction of β - cells. HbA1c is an indicator of chronic glycemic regulation, which rises in the presence of chronic elevated blood glucose levels, which causes non-enzymatic glycation of hemoglobin (Nathan *et al.*, 2008). The resemblance of the control group to the metformins group and selenium group (1.5 mg/kg) indicates that metformin, or low doses of selenium did not appreciably change glucose regulation at long-term as compared to normal animals in the study further describing a highly constant glycemic profile. Nonetheless, the great increase of HbA1c in selenium 5mg/kg-and to a lower level selenium 3 mg/kg-points to the fact that an augmented dosage of selenium diminished glycemic regulation, potentially by heightening insulin sensitivity, sustaining pancreatic β -cell activity, and scuttling oxidative stress-induced β -cell apoptosis (Bajaj *et al.*, 2012). Selenium is associated with endocrine pancreatic health that prevents cellular destruction mediated by ROS as well as enhancing glutathione activity, which is imperative in supporting the existence of the β -cells because of their low intrinsic antioxidant ability (Steinbrenner & Sies, 2013). The efficacy of the 5 mg/kg dose is explained by the reported data that selenium enhances insulin signaling and glucose uptake by activating the antioxidant cascades and maintaining the IRS/PI3K/Akt signaling (Khurana *et al.*, 2019).

The analysis of the present research shows that there are distinct changes in lipid metabolism caused by alloxan where serum cholesterol, triglycerides (TG), and the low-density lipoprotein cholesterol (LDL-C) are highly increased in the alloxan-treated animals relative to all the other experimental groups. Such findings are very consistent with the fact that alloxan has been well-studied to cause not only pancreatic β -cell toxicity but also systemic metabolic dysregulation with lipid homeostasis disturbances induced by oxidative stress and insulin deficiency (El Fouhil *et al.*, 2021; Olatunji *et al.*, 2023). The high increase in all lipid biomarkers in alloxan group implies a drastic dysfunction of lipid clearance mechanisms and increased lipidogenesis in the liver, which are features often seen in diabetic dyslipidemia models. The diabetogenic activity of Alloxan is facilitated by destructive selectivity of the β - cells of the pancreas by generating reactive oxygen species (ROS), which results into sudden decreases of insulin circulating (Szkudelski, 2021). The deficiency of insulin is one of the major causes of dyslipidemia since insulin controls hormone-sensitive lipase, lipoprotein lipase, hepatic very-low-density lipoprotein (VLDL) secretion, and cholesterol metabolism. Lower levels of insulin cause high levels of free fatty acid mobilization of adipose tissue, high levels of VLDL production in the liver, high levels of LDL, and low levels of peripheral clearance of triglyceride-rich lipoproteins (Olatunji *et al.*, 2023). The lipid-lowering properties of selenium in diabetic models are known. There is increased hepatic cholesterol production triggered by high levels of oxidative stress through activation of HMG-CoA reductase and expression of inflammatory cytokines that change lipid metabolism. Selenium improves antioxidant mechanisms and restores metabolic balance to reduce the level of cholesterol in circulation (Ahmad Tarmizi *et al.*, 2024). The remarkable increase of serum triglycerides in the alloxan group in comparison with all other groups is consistent with the literature that indicates that oxidative stress and insulin signaling loss severely decline lipoprotein lipase (LPL) enzyme activity, thus, reducing the ability of lipoprotein lipase to remove triglycerides in circulation (Olatunji *et al.*, 2023; Pereira *et al.*, 2022). Hepatic fatty acid flux, increased de novo lipogenesis, and impaired 2-oxidation are all involved in the increase of TG levels in diabetes. The mechanism by which selenium decreases the triglycerides can be explained by the fact that it can enhance the activity of antioxidant enzymes, reduce lipid peroxidation, and increase the 2-oxidation pathway in mitochondria (Akhtar *et al.*, 2023). Selenium also regulates the expression of lipid-metabolism associated genes, such as peroxisome proliferator-activated receptor alpha (PPAR- 00) enhancing the catabolic of fatty acids and decreasing the hepatic TG storage (Zou *et al.*, 2020).

The histopathological slides of the pancreatic tissue used in the present study indicated that deterioration effects were present in control positive group such as necrosis of β -cells, vacuolar degeneration of serous acini, prominent vascular congestion, and interstitial edema. These results are aligned with the established β -cytotoxic activity of alloxan triggered by rapid ROS formation within cells, the lesion of DNA, as well as the loss of redox homeostasis (Szkudelski, 2021). The mechanism behind Alloxan selective toxicity is explained by the fact that Alloxan is taken up into 2 cell through GLUT2 receptors, which results in oxidative damage and insulin-secreting ability loss. The fact of intense vacuolation of acinar cells is also indicative of acute oxidative damage, a known fact in the pathology of the pancreas in diabetes (Lenzen, 2020). Conversely, pancreatic tissue of animals fed on varying doses of CsSe NPs (1.5mg, 3mg and 5mg/kg.bw) exhibited an effect in the treatment of deleterious effects of Alloxan. The effects of the chitosanselenium nanoparticles were also quite different as compared to those of non-nanoparticle selenium supplementation that had been mentioned in the previous literature. It is known that the bioavailability of CsSe NPs is increased, and their antioxidant activity and cellular uptake are stronger due to the synergistic effects of the advantages of nanoscale selenium and biocompatibility of chitosan (Ahangari *et al.*, 2022). The current findings had a direct reflection of their dose-dependent effects on the pancreatic histology. In the low concentration of Cs NPs (1.5 mg), pancreatic tissue inflamed with the cell infiltration, interlobular duct hypertrophy, and acinar unit degeneration in part. Despite the beneficial effects of nanoparticles on antioxidant activity, inadequate amounts might not be sufficient to address the effects of alloxan-induced oxidative stress. SeNPs at low doses have the potential to induce mild immune responses and potentially free-radical scavenging is not optimal (Zhang *et al.*, 2023). The most significant protection effect was supplied by the largest dose of CsSe NPs (5 mg). Pancreatic sections showed almost normal serous acini, normal interlobular and intralobular ducts, little vascular congestion and only slight fibrosis. The results are in line with the literature that shows that selenium nanoparticles, particularly when stabilized by chitosan, have powerful antioxidant effects, which are manifested through glutathione peroxidase, reduction lipid peroxidation, and inhibition of cords of inflammatory cytokines (Wang *et al.*, 2022; Faisal *et al.*, 2021). Lastly, the histopathological slides of animals that were treated to Metformin had limited degeneration in the islands and almost normal serous acini with congested blood vessels, and normal structure of serous secretory unit (fig7C). Metformin is already known as an antihyperglycemic agent that has anti-oxidants and anti-inflammatory effects that are mediated by the activation of the AMPK, mitochondrial reduction of ROS, and autophagy (Rena *et al.*, 2020; Viollet *et al.*, 2022). The endocrine and exocrine structure is comparatively preserved to aid the presence of metformin in safeguarding of β -cells against oxidative stress and preserving tissue integrity.

CONCLUSION

The chitosan selenium nanoparticles have important antidiabetic, antioxidant and organ protecting effects on alloxan-induced diabetes rats with type 2 diabetes. The effective dosages of CsSe NPs increased, and this clarifies why high doses of CsSe NPs were a promising nanotherapeutic tool in the management of diabetes and its related complications.

REFERENCES

- Aboktifa, M. A., Al-ameedi, A. I., Ayad, Z. M., & Mosa, A. H. (2025). Hepatoprotective properties of piperine in experimentally hepatotoxic male rats exposed to carbon tetrachloride (CCl₄). *J. Anim. Health Prod*, 13(1), 124-128.
- Ahangari, H., Jamshidian, S., & Yaghmaei, P. (2022). Selenium nanoparticles: Properties, applications, and toxicity. *Journal of Nanobiotechnology*, 20(1), 315.
- Ahmad Tarmizi, S. N., Hussin, N., & Wan Ngah, W. (2024). Protective effects of selenium nanoparticles against oxidative stress-induced metabolic dysfunction in diabetic rodents. *Journal of Trace Elements in Medicine and Biology*, 79, 127194.
- Akhtar, S., Khan, M. A., & Aziz, A. (2023). Selenium supplementation attenuates hyperglycemia-induced oxidative stress and dyslipidemia. *Biological Trace Element Research*, 201, 248–259.
- Alissa, E. M., & Ferns, G. A. (2012). Selenium and cardiovascular disease: A review of the evidence. *Eur J Clin Nutr*, 66(6), 593–599. <https://doi.org/10.1038/ejcn.2012.16>
- Al-Quraishy, S., Dkhil, M. A., & Abdel Moneim, A. E. (2015). Anti-hyperglycemic activity of selenium nanoparticles in streptozotocin-induced diabetic rats. *International journal of nanomedicine*, 6741-6756.
- Al-Rekabi, F. K., Alsadawi, A., & Al-Ameedi, A. I. (2021). A New approach in treatment acute ivermectin toxicity in male balb-C mice. *Iraqi Journal of Agricultural Sciences*, 52(2), 301-308.
- AlTamimi, L., Zakaraya, Z. Z., Hailat, M., Ahmad, M. N., Qinna, N. A., Hamad, M. F., & Dayyih, W. A. (2024). Test of insulin resistance in nondiabetic and streptozotocin-induced diabetic rats using glycosylated hemoglobin test and other interventions. *Journal of Advanced Pharmaceutical Technology & Research*, 15(1), 1-7.
- Bajaj, S., Khan, A. A., & Saluja, R. (2012). Effect of selenium supplementation on oxidative stress and insulin secretion in streptozotocin-induced diabetic rats. *Biol Trace Elem Res*, 148(2), 215–221.
- Barchielli, G., Capperucci, A., & Tanini, D. (2022). The role of selenium in pathologies: an updated review. *Antioxidants*, 11(2), 251.
- Bîrsan, V. G., Dimitriu, L., Șomoghi, R., Berger, D., Aruxandei, D. C., & Oancea, F. (2022). Synthesis and Characterization of Medium Molecular Weight Chitosan-Stabilized Selenium Nanoparticles. *Chemistry Proceedings*, 7(1), 85.
- Bugianesi, E., McCullough, A. J., & Marchesini, G. (2005). Insulin resistance: A metabolic pathway to chronic liver disease. *Hepatology*, 42(5), 987–1000.
- Chen, X., Zhang, Z., Gu, M., Li, H., Shohag, M. J. I., Shen, F., ... & Wei, Y. (2020). Combined use of arbuscular mycorrhizal fungus and selenium fertilizer shapes microbial community structure and enhances organic selenium accumulation in rice grain. *Science of the Total Environment*, 748, 141166.
- Das, U., Mali, S. N., & Mandal, S. (2025). Unveiling the Ameliorative Effects of Phyto-Selenium Nanoparticles (PSeNPs) on Anti-Hyperglycemic Activity and Hyperglycemia Irradiated Complications. *BioNanoScience*, 15(2), 231.
- DeDiego, M. L., Portilla, Y., Daviu, N., López-García, D., Villamayor, L., Vázquez-Utrilla, P., ... & Barber, D. F. (2024). Biocompatible Iron Oxide Nanoparticles Display Antiviral Activity Against Two Different Respiratory Viruses in Mice. *International journal of nanomedicine*, 13763-13788.
- Desouky, M. M., Abou-Saleh, R. H., Moussa, T. A., & Fahmy, H. M. (2025). Nano-chitosan-coated, green-synthesized selenium nanoparticles as a novel antifungal agent against Sclerotinia sclerotiorum: in vitro study. *Scientific Reports*, 15(1), 1004.
- Dnan GD, Al-Awadi HK, Al-Ameedi AI (2025). Gallic acid and olive oil ameliorate atherosclerosis in experimentally induced in male rats. *J. Anim. Health Prod*. 13(s1): 422-427.
- El Fouhil, A. F., Nasser, A. A., & El Masry, S. A. (2021). Dyslipidemia in experimental diabetes: Mechanisms and therapeutic approaches. *Diabetes & Metabolic Syndrome*, 15(1), 249–257.
- Faisal, M., Saquib, Q., & Alatar, A. (2021). Chitosan-based selenium nanoparticles: Antioxidant and anti-inflammatory potential. *Carbohydrate Polymers*, 251, 117106.
- Forbes, J. M., & Cooper, M. E. (2013). Mechanisms of diabetic complications. *Physiological Reviews*, 93(1), 137–188.
- Giacco, F., & Brownlee, M. (2010). Oxidative stress and diabetic complications. *Circulation Research*, 107(9), 1058–1070.
- Hatfield, D. L., Tsuji, P. A., Carlson, B. A., & Gladyshev, V. N. (2014). Selenium and selenocysteine: Roles in cancer, health, and development. *Trends Biochem Sci*, 39(3), 112–120.
- Huang, Z., Rose, A. H., & Hoffmann, P. R. (2012). The role of selenium in inflammation and immunity: From molecular mechanisms to therapeutic opportunities. *Antioxid Redox Signal*, 16(7), 705–743.
- Ibrahim, O., Ayad, Z. M., & Omar, L. W. (2018). Efficacy of Silver Nanoparticles, Antimicrobial peptides and Blue Light Combination on Healing Infected Wound by Methicillin Resistance *Staphylococcus aureus* in Rats. *Kufa Journal For Veterinary Medical Sciences*, 9(2).

- Karim, R., Abdullah, M., & Rahman, S. (2024). Selenium nanoparticles improve lipid metabolism and reduce oxidative LDL in diabetic rats. *Nanomedicine*, 48, 102695.
- Khurana, S., et al. (2019). Selenium supplementation enhances insulin signaling and reduces oxidative stress in diabetic rats. *Nutrients*, 11(9), 2101. <https://doi.org/10.3390/nu11092101>
- Klapetek, P., Valtr, M., Nečas, D., Salyk, O., & Dzik, P. (2011). Atomic force microscopy analysis of nanoparticles in non-ideal conditions. *Nanoscale research letters*, 6(1), 514.
- Lenzen, S. (2008). The mechanisms of alloxan- and streptozotocin-induced diabetes. *Diabetologia*, 51(2), 216–226.
- Lenzen, S. (2020). Oxidative stress: The vulnerable renal and endocrine tissue. *Biochemical Society Transactions*, 48(4), 1099–1107.
- Li, Y., Lin, Z., & Zhao, M. (2020). Chitosan-stabilized selenium nanoparticles enhance antioxidant activity and improve bioavailability. *Carbohydrate Polymers*, 228, 115365.
- Lin, Z.H. and Chris Wang, C.R. Evidence on the Size-Dependent Absorption Spectral Evolution of Selenium Nanoparticles. *Material Chemistry Physics*. 2005. 92; 591-594.
- Malik, Z. J., Alameedi, A. I., & Abdulah, M. (2022). The effects of common carp, *Cyprinus carpio* skin collagen extract on infected wounds. *Iranian Journal of Ichthyology*, 9, 104-109.
- Mohamed, A. A. R., Khater, S. I., Arisha, A. H., Metwally, M. M., Mostafa-Hedeab, G., & El-Shetry, E. S. (2021). Chitosan-stabilized selenium nanoparticles alleviate cardio-hepatic damage in type 2 diabetes mellitus model via regulation of caspase, Bax/Bcl-2, and Fas/FasL-pathway. *Gene*, 768, 145288.
- Nathan, D. M., Kuenen, J., Borg, R., Zheng, H., Schoenfeld, D., & Heine, R. J. (2008). Translating the A1C assay into estimated average glucose values. *Diabetes Care*, 31(8), 1473–1478.
- Olatunji, L. A., Adedosu, T., & Salako, A. (2023). Alloxan-induced diabetes and metabolic dysregulation: New insights into oxidative mechanisms. *Journal of Diabetes Research*, 2023, 5598123.
- Pereira, R., Pinto, A. L., & Silva, C. (2022). Triglyceride metabolism in diabetes: The role of oxidative stress and lipoprotein lipase. *Metabolism Open*, 14, 100181.
- Rahmanto, A. S., & Davies, M. J. (2012). Selenium and oxidative stress: Implications for diabetes. *Free Radic Biol Med*, 53(9), 1696–1708.
- Ramamurthy, C. H., Padma, M., Mareeswaran, R., Suyavaran, A., Kumar, M. S., Premkumar, K., & Thirunavukkarasu, C. (2013). The extra cellular synthesis of gold and silver nanoparticles and their free radical scavenging and antibacterial properties. *Colloids and Surfaces B: Biointerfaces*, 102, 808-815.
- Rena, G., Hardie, D. G., & Pearson, E. R. (2017). The mechanisms of action of metformin. *Diabetologia*, 60(9), 1577–1585.
- Rena, G., Hardie, D. G., & Pearson, E. R. (2020). Mechanisms of metformin action. *Diabetologia*, 63, 2134–2145.
- Rolo, A. P., & Palmeira, C. M. (2006). Diabetes and mitochondrial function: Role of hyperglycemia and oxidative stress. *Toxicol Appl Pharmacol*, 212(2), 167–178.
- Solini, A., & Tricò, D. (2024). Clinical efficacy and cost-effectiveness of metformin in different patient populations: A narrative review of real-world evidence. *Diabetes, Obesity and Metabolism*, 26, 20-30.
- Steinbrenner, H., & Sies, H. (2013). Selenium homeostasis and antioxidant selenoproteins in health and disease. *Free Radical Biology & Medicine*, 65, 1–12.
- Szkudelski, T. (2001). The mechanism of alloxan and streptozotocin action in pancreatic β -cells. *Physiological Research*, 50(6), 537–546.
- Szkudelski, T. (2021). Alloxan as a model toxin in diabetic and renal studies. *Journal of Physiology and Pharmacology*, 72(5), 651–667.
- Viollet, B., Guigas, B., & Foretz, M. (2022). Metformin as a regulator of oxidative metabolism. *Trends in Endocrinology & Metabolism*, 33(3), 156–170.
- Viollet, B., Guigas, B., Garcia, N. S., Leclerc, J., Foretz, M., & Andreelli, F. (2012). Cellular and molecular mechanisms of metformin: An overview. *Clin Sci*, 122(6), 253–270.
- Wang, Y., Guo, X., & Li, Z. (2022). Selenium nanoparticles in oxidative stress protection: Mechanisms and biomedical potential. *Antioxidants*, 11(2), 345.
- Wongdokmai, R., Shantavasinkul, P. C., Chanprasertyothin, S., Panpunuan, P., Matchariyakul, D., Sritara, P., & Sirivarasai, J. (2021). The involvement of selenium in type 2 diabetes development related to obesity and low grade inflammation. *Diabetes, Metabolic Syndrome and Obesity*, 1669-1680.
- Ye, R., Huang, J., Wang, Z., Chen, Y., & Dong, Y. (2021). Trace element selenium effectively alleviates intestinal diseases. *International Journal of Molecular Sciences*, 22(21), 11708.
- Zeng, H., Uthus, E. O., & Combs, G. F., Jr. (2008). Selenium as an antioxidant and its role in diabetes. *J Nutr Biochem*, 19(10), 694–703.
- Zhang, J., Wang, X., & Xu, T. (2023). Dose-dependent antioxidant and anti-inflammatory activity of selenium nanoparticles. *International Journal of Nanomedicine*, 14, 7149–7160.